Talanta 76 (2008) 1029–1034

Contents lists available at ScienceDirect

Talanta

journal homepage: www.elsevier.com/locate/talanta

Brewster angle microscopic study of mixed lipid–protein monolayer at the air–water interface and its application in biosensing

A.K.M. Kafi*, Young-Soo Kwon**

Department of Electrical Engineering & NTRC, Dong-A University, 840 Hadan-2dong, Saha-gu, Busan 604-714, Republic of Korea

ARTICLE INFO

Article history:
Received 20 February 2008
Received in revised form 28 April 2008
Accepted 30 April 2008
Available online 8 May 2008

Keywords:
BAM
Protein
Lipid
Biosensor

ABSTRACT

This study investigated lipid–protein LB film formation with Brewster angle microscopy. Our experimental results show that hemoglobin (Hb) molecules can enter the lipid layer and remain for an extended time. We investigated the KCl effect on the LB monolayer of lipid–protein. The lipid–Hb monolayer was transferred from the air–water interface to a QCM gold electrode. UV–vis spectra showed that Hb retained its natural structure in the lipid layer. Cyclic voltammetric (CV) and amperometric systems were applied in this study in order to confirm the remaining bioactivity and sensitivity of Hb to hydrogen peroxide (H_2O_2). Lipid–Hb-modified electrodes showed well-defined redox peaks, indicating that the direct electron transfer between Hb and the electrode was enhanced by Hb incorporated in lipid layer. Based on this phenomenon, a novel biosensor for H_2O_2 was designed. Experimental conditions influencing the biosensor performance such as pH, and potential were optimized and assessed. The levels of the R.S.D.'s (<5%) for the entire analyses reflected the highly reproducible sensor performance. Using optimized conditions the linear range for the detection of H_2O_2 was observed from 1×10^{-6} to 1.00×10^{-4} mol L^{-1} with a detection limit of 4.00×10^{-7} mol L^{-1} (based on the S/N = 3).

1. Introduction

The behavior of protein adsorption on different matrices and the interaction and direct electron transfer between proteins and the electrode surfaces are of great importance in electrocatalytic biosensing [1]. Langmuir–Blodgett (LB) technique offers the possibility of developing an ultra-thin film with well-organized structure on the molecular scale [2]. As well, this technique is considered as a suitable immobilization method for biosensor manufacture given its applicability to creating uniform, well-ordered thin films with the amount of biocomponents controlled by varying the number of deposited layers. LB technique has previously been used to immobilize various biomolecules [3–7]. One of the emerging fields of application of LB film is the development of organized protein or enzyme layers for biosensors and for various analytical techniques [8]. The potentiality of two-dimensional LB monolayer of lipid molecules, which have been extensively used as a part of designing sensitive biosensor [9,10]. It is very important for the electroactivity of a protein or enzyme to be conserved on the solid surface. Normally proteins or enzymes have high molecular weight, large relative size, and a very flexible structure that can change conformation according to the experimental and immobilization conditions. A number of methods have been used to form protein/enzyme monolayers to protect the denaturization of its activity during the fabrication of biologically active films [8,11,12].

As part of the research interests of our lab, we already report the formation of protein layers by various matrix preparations, including LB technique, all applied to direct electron transfer processes [9,10,13]. It is noteworthy that the conventional method for forming lipid–protein film is to first dissolve proteins in subphase firstly, then dispersing lipid onto the subphase surface. There are problems associated with this system such as the unwanted formation of a passive layer prior to film deposition which can impact the electron transfer activity of protein. To solve this problem, we already have reported a new method of forming lipid–protein film [9,10].

In the present study, the above-mentioned method was applied to the formation of Hb–lipid monolayer at the water–air surface and deposition onto the solid substrate. A number of biosensors have been designed based on Hb in various configurations [14–18]. The redox centre of Hb is electrically insulated by a relatively thick protein shell, hindering its direct electrical communication with an electrode, yet it is very important for this molecule to maintain its electroactivity on the electrode surface [19]. We seek to overcome this problem by using LB technique [9,10,20]. The approach

* Corresponding author. Current address: Department of Chemistry, Lakehead University, Thunder Bay, Ontario P7B 5E1, Canada. Tel.: +1 807 343 850; fax: +1 807 346 7775.
** Corresponding author.
E-mail addresses: akafi@lakeheadu.ca (A.K.M. Kafi), yskwon@dau.ac.kr (Y.-S. Kwon).

0039-9140/$ – see front matter © 2008 Elsevier B.V. All rights reserved.
doi:10.1016/j.talanta.2008.04.061

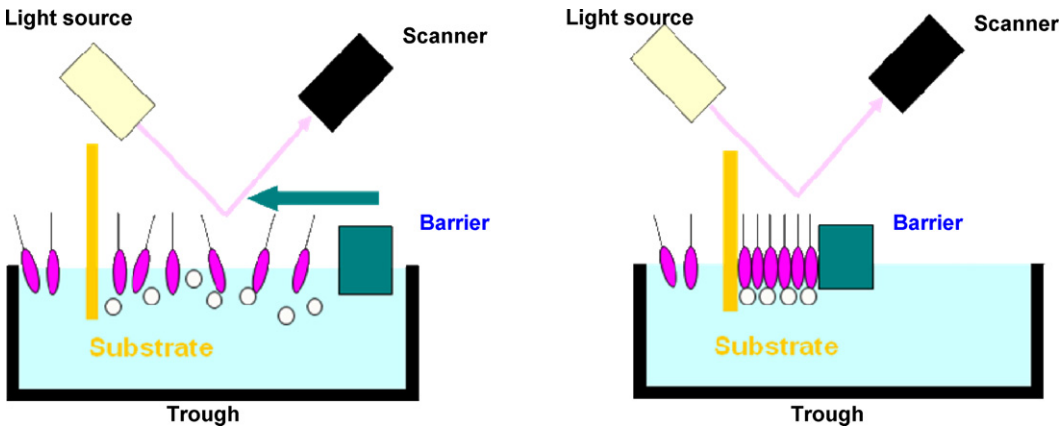

Fig. 1. The schematic figure of BAM image during Hb–LA LB film formation at air–water interface.

we propose for making Hb–lipid LB film was expected to enhance performance of Hb electron transfer activity at the electrode. Finally this Hb–lipid film was applied as a biosensor for detecting H_2O_2.

Hemoglobin is a promising biomaterial for the study of electron transfer reactions of proteins and for designing biosensors [13,16–18]. Reports have been published on the incorporation of Hb in different membranes or microenvironments [21–23], but the study of Hb with lipid film at the air–water interface has received scant attention. Lipid monolayers have been used as an adsorption layer for deposition of nanoparticles [24,25], salts [26], clay [27], or enzymes [28] from the aqueous phase. The performances of protein adsorbed onto the matrix monolayer at the air–water interface has been observed using fluorescence spectra, ellipsometry, surface plasmon resonance, etc. [29]. In this regards, Brewster angle microscopy (BAM) was first used to study monolayer in the early 1990s [30]. With the implementation of BAM for monolayer characterization, it has become possible to visualize the inner structure of different stages of lipid–protein LB film at the air–water interface without the requirement of added probes [1]. It is noteworthy that the conventional method for forming lipid–protein film is to dissolve proteins in subphase first, proceeded by dispersion of lipid onto the surface of subphase. There are problems associated with this system that affect the electron transfer activity of protein such as the creation of a passive layer before film deposition. To solve this problem, we already have reported a new method of forming lipid–protein film [9,10].

Reported for the first time in this paper are the formation of Hemoglobin (Hb)–lauric acid (LA) LB films characterized with BAM study. Specifically the formation of Hb–LA film has been observed using BAM. After depositing this film onto the Au surface, electrochemical properties were investigated. Our experimental data showed that this type of highly uniform film has good potential as a recognition layer for biosensing. As an extension of this the film possessed good electrocatalytic properties towards H_2O_2.

2. Experimental

2.1. Reagents

Hemoglobin was purchased from Sigma and used as received. Lauric acid (LA) was obtained from Aldrich. Stock solutions of H_2O_2 were diluted from 30% solution. All other reagents were of analytical grade and were used as supplied. The experimental solutions were freshly prepared each day by appropriate dilution of the stock solutions. Stock solutions were stored at a temperature of 4 °C. All stock solutions were made using freshly double distilled water. Water (18 MΩ cm) was purified using the Nanopure water system and was used to prepare all solutions. All experiments were performed in 0.1 M phosphate buffer solution (PBS) prepared from K_2HPO_4 and KH_2PO_4 then adjusted to desired pH by adding HCl.

2.2. LB film formation and BAM investigation

Fig. 1 shows a schematic BAM image taken of Hb–LA LB film forming at the air–water interface. LA (chloroform solution, 1 mg/ml) was spread onto the interface of subphase containing 1.0 M KCl and 0.001 mM PBS in a Langmuir–Blodgett through together with Multiskop (Optrel, German). The surface pressure was measured using a Wilhelmy balance equipped with a strip of chromatography paper suspending at the air–water interface. Surface pressure data along with trough and molecular areas are fed and recorded directly into a computer. After LA solution was spread onto the subphase interface for a minimum of 10 min, Hb solution (0.5 mg/ml, pH 7.0 phosphate buffer) was spread carefully onto the subphase, covered with a layer of LA. A pressure–surface area (π–A) curve was immediately recorded to evaluate the state of Hb/LA layer. BAM images were also concurrently recorded. The mixed Hb–LA layer was deposited from LB trough to a 9 MHz AT-cut PQC with gold electrode substrate. The monolayer of Hb–LA on substrate surface was obtained under controlled surface pressures using vertical withdrawal method, keeping 5 mm min^{-1} as the withdrawal speed. Prior to electrochemical measurements, Hb–LA-modified gold electrode was thoroughly washed with ultra-pure water. The modified electrode was kept at 4 °C when not in use. Only LA-modified gold electrode was fabricated in the same way. The electrodes will be referred to from this point on as Au–Hb–LA and Au–LA electrode, respectively.

2.3. Instrumentation and electrochemical measurements

The UV–vis spectrum was measured using a PerkinElmer UV–vis spectrometer. Cyclic voltammetry and amperometry were carried out with the CHI630 (B) workstation. A three-electrode system was employed in these experiments. A quartz crystal microbalance gold electrode was used as the mass loading substrate and working electrode following cleaning with a piranha solution. Cyclic voltammetry (CV) experiments were carried out in 0.1 M PBS by applying 0.3–−0.7 V vs. Ag/AgCl sweep range in the negative scanning direction. Amperometric measurements were carried out in a stirred cell by applying a potential of −500 mV to the working electrode. Prior to each experiment, the electrolyte solution was purged with high purity nitrogen for a minimum of

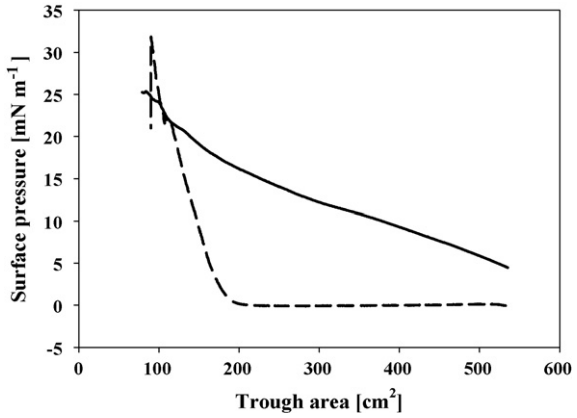

Fig. 2. π–A isotherm of lipid-only (LA) (dashed line) and lipid–Hb film (solid line) on subphase.

30 min. An inert environment was maintained during electrochemical measurements by allowing a gentle flow of nitrogen through the cell. A magnetic stirrer was employed during amperometry experiments. All measurements were performed at room temperature.

3. Results and discussion

3.1. LB film formation and BAM

Fig. 2 shows the typical pressure–area (π–A) isotherm of lipid and lipid–Hb Langmuir film onto a subphase of KCl solution in pure water. As can be seen in this figure, after spreading Hb molecule onto the subphase surface covered with lauric acid, the initial surface pressure increased immediately. This would indicate that already some Hb molecules have entered the lipid layer. We have investigated the effect of KCl concentration on the formation of lipid–Hb LB monolayer. Maximum increase of initial surface occurred at a 1.0 M KCl concentration. It is at this point that the maximum amounts of Hb molecules enter into the lipid layer. For this reason 1.0 M concentration of KCl was chosen as the optimal condition for forming lipid–Hb LB film.

Fig. 3 shows the BAM images along with π–A isotherm of lipid-only LB monolayer in the different states. Fig. 3(a) shows the BAM image of only lipid layer after solvent evaporation (chloroform) just prior to the start of barrier compression. In this image are visible clear white dots predicted to be lipid molecule. Fig. 3(b) shows a BAM image of same lipid film when surface pressure of the monolayer was approx. 15 mN/m. In this figure the white dots are seen to be approaching each other forming a colony type of film. Finally, in Fig. 3(c), we can observe the highly organized monolayer of LB–lipid film. This BAM image was taken at a surface pressure of approx. 25 mN/m. From this we can ascertain that the lipid will form a well packed LB film monolayer when the surface pressure reaches approx. 25 mN/m. Fig. 4 shows BAM images of lipid–Hb monolayer along with π–A isotherm obtained when Hb was spread onto lipid covered subphase. Fig. 4(a) shows the BAM image of lipid–Hb monolayer just after spreading Hb molecules onto the lipid film. The surface pressure was approx. 4 mN/m. In this figure can be discerned bright dots along with patch-like black spots. In Fig. 4(b) the black spots are more clearly visible and presumed to be Hb molecules. Fig. 4(c) shows the same lipid–Hb LB film at a surface pressure of approx. 25 mN/m. It is of interest to note that the black spots are more clearly observed in this picture. In contrast the white dots are less aggregated than in the lipid-only film of Fig. 3(b) at identical surface pressures. From this set of observations we can characterize the black patch-like spots as being Hb molecule. Thus, it can be concluded that Hb molecule entered the lipid layer and formed a well-defined lipid–Hb layer. We observed similar images after 2 h resting time suggesting that the lipid–Hb LB film has long time stability.

3.2. UV study of the LB film

For this experiment, the lipid–Hb film was transferred onto quartz at a surface pressure of 20 mN/m controlled by maintaining a withdrawal speed of 5 mm min^{-1}. Only lipid film was also deposited onto the quartz under same conditions. After depositing this film quartz, the UV–vis properties were investigated. To characterize the native structure of Hb in lipid film we investigated the UV–vis spectra. According to Fig. 5, UV–vis spectra of mixed Hb–lipid showed almost identical absorption pattern as Hb alone in solution (maximum absorption was at approx. 428 nm). The results illustrate that Hb keeps its native structure in LA film.

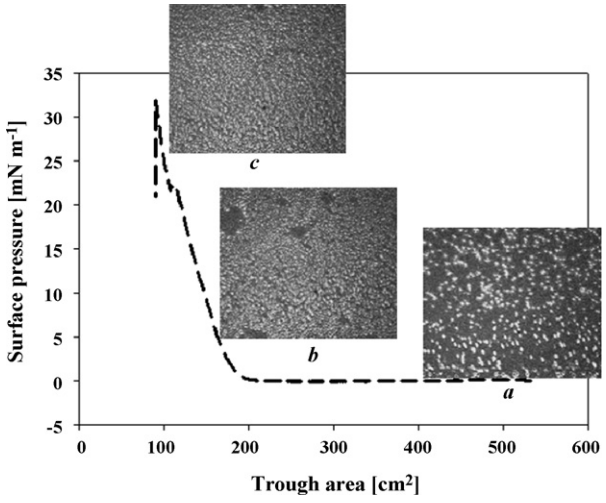

Fig. 3. BAM image of lipid-only LB film at different surface pressures: (a) surface pressure is 0 mN/m, (b) surface pressure is 15 mN/m and (c) surface pressure is 25 mN/m.

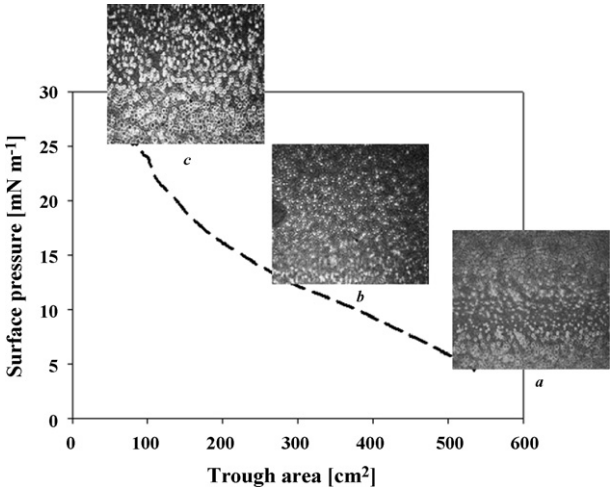

Fig. 4. BAM image of lipid–Hb LB film at different surface pressures: (a) surface pressure is 0 mN/m, (b) surface pressure is 15 mN/m and (c) surface pressure is 25 mN/m.

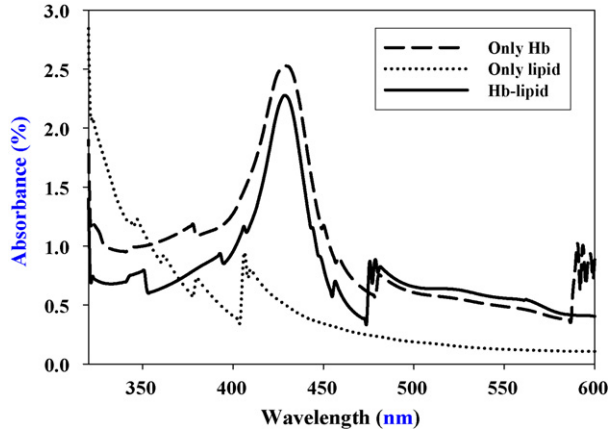

Fig. 5. UV of LA-only (dotted line), Hb-only (dashed) and LA–Hb-modified gold electrode.

3.3. Electrochemistry of LB film

Fig. 6 compares the cyclic voltammograms of the Au–Hb–LA and Au–LA electrode. It can be observed that there is a pair of well-defined redox peaks (solid line) at the Au–Hb–LA-modified electrode in 0.1 PBS (7.0). In contrast, no peak was observed at the Au–LA (dashed line) electrode under same experimental conditions. This comparison verifies that the redox peak arises from the electrochemical reaction of Hb. The result also establishes that direct electron transfer between Hb and the electrodes has occurred. The anodic and cathodic peak potentials for Hb are located at approx. −260 and −40 mV. The formal potential, E_0, was calculated to be −150 mV. Normally, Hb does not show electroactivity at the bare electrode [22]. Therefore, it can be established that Au–Hb–LA electrode plays an important role in enhancing electron transfer rate between the Au electrode and Hb. From this it can also be gathered that lipid layer provides a good matrix for Hb immobilization and biosensor fabrication. Fig. 7 shows the effect of scanning rate on the Au–Hb–LA electrode response. It was found that with an increase of scan rate from 50 to 200 mV/s the redox peak currents of Hb increased linearly. It should also be noted that peak-to-peak separation increased with increasing scan rates. The experimental data proves that this is a quite quasi-reversible and surface-controlled redox process [13].

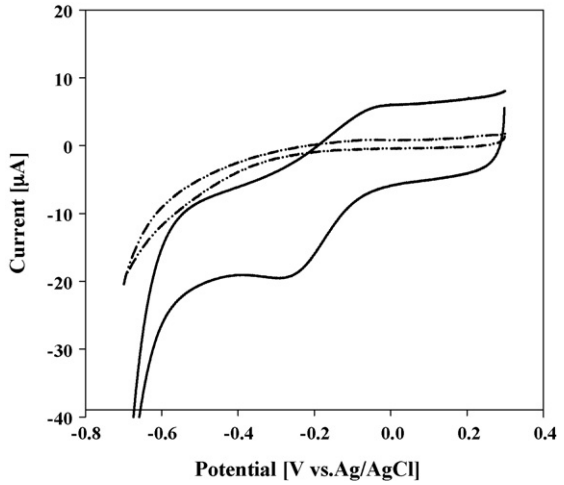

Fig. 6. CV graphs of LA-only (dashed line) and LA–Hb-modified gold electrode (solid line) (scan rate was 100 mV/s).

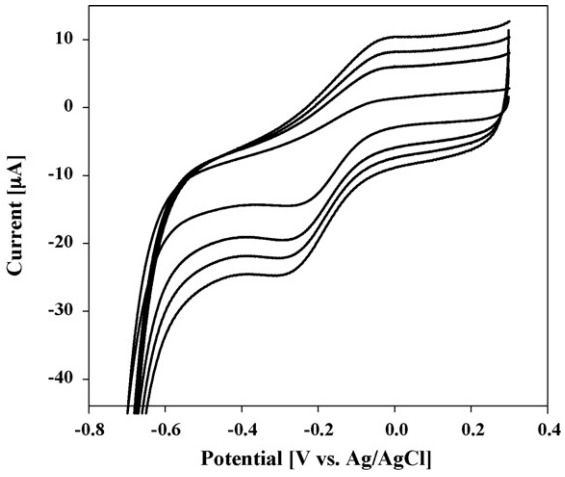

Fig. 7. CV graphs of LA–Hb-modified gold electrode (with different scan rate).

3.4. Electrocatalytic activity towards H_2O_2

Fig. 8 shows typical cyclic voltammograms (CVs) of the Au–Hb–LA electrode in the absence of and in the presence of 1.0×10^{-4} mol L^{-1} H_2O_2 in 0.1 M PBS at pH 7.0. As shown in Fig. 8 when 1.0×10^{-4} mol L^{-1} H_2O_2 is added to PBS, a marked increase in peak reduction current was observed accompanied by a decrease in the oxidation peak, providing an indication of the electrocatalytic properties of the modified electrode. It can be confidently stated that the catalytic reduction of H_2O_2 is due to hemoglobin immobilized in lipid film. We suggest that this type of lipid–Hb film can be used for biosensor fabrication. The generic reaction occurring at the electrode is given by the following equation [16]:

$$Hb(Fe^{III}) + H^+ + e^- \; Hb(Fe^{II}) \quad (1)$$

3.5. Optimization of experimental parameters

The effect of applied potential on the amperometric response of the biosensor is an important parameter. We investigated the influence of applied potential on the current response of the Au–Hb–LA electrode surface to H_2O_2. Fig. 9(A) shows the current response at different applied potentials in the presence of 2.0×10^{-5} mol L^{-1} H_2O_2 in a pH 7.0 PBS. This data reveals that the steady-state reduction current increases gradually as the voltage decreases from

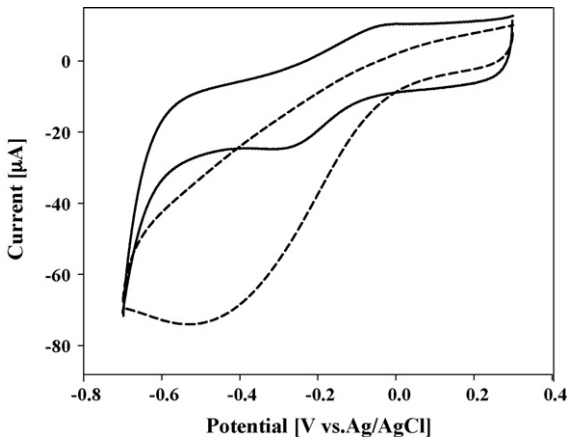

Fig. 8. CV graphs of the LA–Hb-modified gold electrode in the presence of 1.0×10^{-4} mol L^{-1} H_2O_2 in 0.1 M PBS at pH 7.0 (solid line) and the absence (dashed line) of H_2O_2 (scan rate was 100 mV/s).

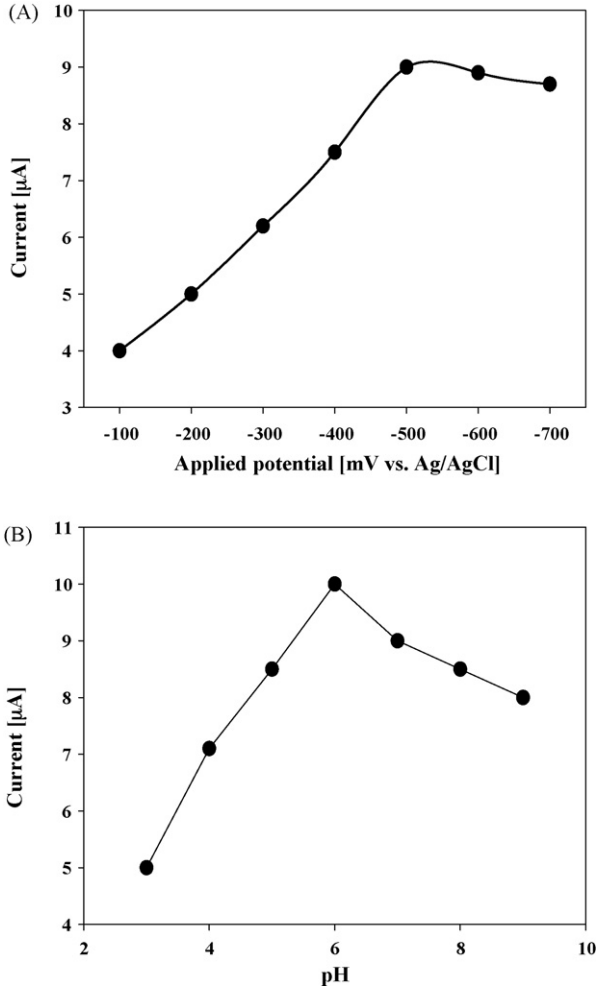

Fig. 9. (A) Dependence of biosensor catalytic current on applied potentials in the presence of 2.0×10^{-5} mol L^{-1} H_2O_2 in a pH 7.0 PBS. (B) Influence of pH on biosensor catalytic current in the presence of 2.0×10^{-5} mol L^{-1} H_2O_2 at a potential of −500 mV.

−100 to −500 mV. The maximum reduction current was achieved at −500 mV. At more negative potential risk of interference from other electroactive species may be involved. With this in mind we chose a working potential of −500 mV for this biosensor, where the background current is minimized and any unforseen interference reactions of other electroactive species can be effectively avoided.

The influence of pH value is another important factor on the response of electrolytic H_2O_2 biosensors. The effect of pH on biosensor response in the presence of H_2O_2 was investigated for the electrodes in question. Fig. 9(B) shows the amperometric current response of the Au–Hb–LA-electrode at different pH in the presence of 2.0×10^{-5} mol L^{-1} H_2O_2. An increase in amperometric current corresponded to an increase in pH from 3.0 to 6.0; however, the amperometric response decreased when pH was further increased from 7.0 to 9.0. In lower pH values (<4.0) the current response is very low. At these pH values the low response may be due to denaturation of the biomolecule [31]. As the maximum response current in this experiment was observed at pH 6.0, this pH was chosen as a working pH for the following experiment.

3.6. Amperometric response of the biosensor

Investigation of the amperometric response of the Au–Hb–LA-electrode was performed in a stirred cell containing 0.1 M PBS (pH 6.0) at an operating potential of −500 mV. Fig. 10 shows the typical current-response at Au–Hb–LA-electrode for successive addition of H_2O_2. Observe that as soon as H_2O_2 was added, the background current changed and the reduction current rose steeply to reach maximum value. The response of the fabricated biosensor to H_2O_2 is very quick; over 95% of the steady-state current was achieved within 5 s. Increasing the H_2O_2 concentration resulted in a proportional increase of the amperometric response.

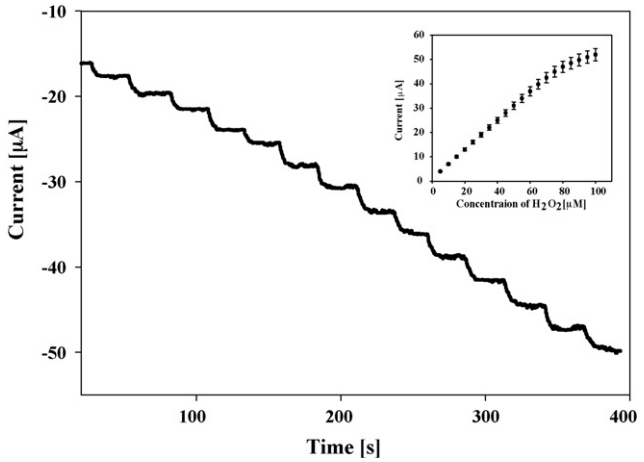

Fig. 10. Typical current–time response of LA–Hb-modified gold electrode with total additions of 1×10^{-4} mol L^{-1} H_2O_2 in 0.1 M PBS (pH 6.0) at an operating potential of −500 mV (inset, the calibration plot of the biosensor based on Fig. 10).

Fig. 10 (inset) shows the calibration plots obtained for the Au–Hb–LA-electrode electrode using optimum experimental conditions. Under optimal conditions, the proposed biosensor displays a linear range for H_2O_2 determination from 1×10^{-6} to 1.00×10^{-4} mol L^{-1} with a correlation coefficient of 0.996 ($n = 14$). The detection limit of the proposed biosensor was estimated to through the S/N = 3 is 4×10^{-7} mol L^{-1}.

3.7. Selectivity and stability of the biosensor

We also investigated the effect of a select number of substances that interfere with the response of the proposed biosensor. Analytes were added to the PBS containing 0.2 mM H_2O_2. The current inhibition was obtained for each interfering substance present at a concentration of 0.2 mM. Glucose, acetic acid, ethanol, and citric acid caused no observable interference. In the case of ascorbic acid, the initial value of current response decreased by 20%. This effect was presumably due to the consumption of H_2O_2 through oxidation of ascorbic acid [32]. The long-term stability of this biosensor was also investigated. The Au–Hb–LA-electrode was stored in PBS (pH 7.0) at 4 °C when not in use. It retained 85% of its initial current response after being stored for 35 days. The repeatability of the sensor's current response was also examined. It was found that the relative standard deviation (R.S.D.) was 4.75% for ten successive measurements at a H_2O_2 concentration of 2×10^{-5} μM.

4. Conclusion

We have observed the Brewster angle microscopic image of hemoglobin in lipid film at the air–water interface. The BAM results illustrate that hemoglobin molecules can enter lipid film and remain for an extended time. Cyclic voltammetric results showed there is a well-defined redox peak attributed to the redox heme centre of Hb. UV–vis spectra showed that Hb keeps its native structure in lipid layer following deposition to the electrode surface. In addition, this kind of film is promising for biosensor design. Based

on LA–Hb film, a hydrogen peroxide biosensor was designed. Our experimental data showed that this LB film could be employed as a functional H_2O_2 detector. As a biosensor it shows long linear range and low detection limit. The combination of low detection limit, long linear range and high stability are obvious advantages of this biosensor. This present work will further guide us towards an understanding of the redox characteristics of enzymes in lipid matrix at the air–water interface.

Acknowledgment

This work was supported by the Korean Science and Engineering Foundation (KOSEF) grant funded by the Korean government (MOST) (No. R01-2006-000-11120-0).

References

[1] Z. Zhang, R.S. Magliozzo, J.F. Rusling, Anal. Chem. 74 (2002) 163.
[2] G.G. Roberts, Langmuir Blodgett Films, Plenum, New York, 1990.
[3] J.M. Chovelon, M. Provence, N. Jaffrezic-Renault, N.V. Derue, D. Lair, S. Alexandre, J.M. Valleton, J. Biol. Phys. Chem. 1 (2001) 68.
[4] J.M. Chovelon, M. Provence, N. Jaffrezic-Renault, Langmuir 16 (2000) 6228.
[5] A. Zhang, A. Jafferezic-Renault, J. Wan, Y. Hou, J.M. Chovelon, Mater. Sci. Eng. 21 (2002) 91.
[6] G.K. Chudinova, A.V. Chudinov, V.V. Savransky, A.M. Prokhorov, Thin Solid Films 307 (1997) 294.
[7] A. Barraud, H. Perrot, V. Billard, C. Martelet, J. Therasse, Biosens. Bioelectron. 8 (1993) 39.
[8] M. Aizawa, K. Owaku, M. Matsuzawa, H. Shinorhara, Y. Ikariama, Thin Solid Films 180 (1989) 227.
[9] F. Yin, H.-K. Shin, Y.-S. Kwon, Talanta 67 (2005) 221.
[10] F. Yin, A.K.M. Kafi, H.-K. Shin, Y.-S. Kwon, Thin Solid Films 488 (2005) 223.
[11] Y. Okahata, T. Tsuruta, K. Ijiro, K. Ariga, Thin Solid Films 180 (1989) 65.
[12] S.Y. Zaitsev, Colloid Surf. 75 (1993) 211.
[13] A.K.M. Kafi, D.-Y. Lee, S.-H. Park, Y.-S. Kwon, J. Nanosci. Nanotechnol. 6 (2006) 3539.
[14] H. Hang, R. Guan, C. Fan, D. Zhu, G. Li, Sens. Actuators B 84 (2002) 214.
[15] F. Zhao, X. Wu, M. Wang, Y. Liu, L. Gao, S. Dong, Anal. Chem. 76 (2004) 4960.
[16] S. Liu, Z. Dai, H. Chen, H. Ju, Biosens. Bioelectron. 19 (2004) 963.
[17] Y.D. Zhao, Y.H. Bi, W.D. Zhang, Q.M. Luo, Talanta 65 (2005) 489.
[18] Y. Wang, W. Qian, Y. Tan, S. Ding, H. Zhang, Talanta 72 (2007) 1134.
[19] B.Q. Wang, J.Z. Zhang, G.J. Cheng, S.J. Dong, Anal. Chim. Acta 407 (2000) 111.
[20] K. Wan, J.M. Chovelon, N.J. Renault, Talanta 52 (2000) 663.
[21] J.H. Sun, N.F. Hu, H.Y. Ma, Electroanalysis 12 (2002) 1064.
[22] A.-E.F. Nassar, J.F. Rusling, J. Am. Chem. Soc. 118 (1996) 3043.
[23] Q.D. Huang, Z.Q. Lu, J.F. Rusling, Langmuir 12 (1996) 5472.
[24] K. Muramatsu, M. Takahashi, K. Tajima, K. Kobayashi, J. Colloid Interf. Sci. 242 (2001) 127.
[25] H. Du, Y.B. Bai, Z. Hui, L.S. Li, Y.M. Chen, X.Y. Tang, T.J. Li, Langmuir 13 (1997) 2538.
[26] P. Ganguly, D. Paranjape, V. Sastry, Langmuir 9 (1993) 574.
[27] R.H.A. Ras, C.T. Johnston, E.I. Franses, R. Ramaekers, G. Maes, P. Foubert, F.C. De Schryver, R.A. Schoonheydt, Langmuir 19 (2003) 4295.
[28] J. Jin, L.S. Li, X. Wang, Y. Li, Y.J. Zhang, T.J. Li, Langmuir 15 (1999) 6969.
[29] T. Kondo, T. Kakiuchi, M. Shimomura, Thin Solid Films 244 (1994) 887.
[30] S. Henon, J. Meunier, Rev. Sci. Instrum. 62 (1991) 936.
[31] X. Chen, N. Hu, Y. Zeng, J.F. Rusling, J. Yang, Langmuir 15 (1999) 7022.
[32] A.K.M. Kafi, D.-Y. Lee, S.-H. Park, Y.-S. Kwon, Microchem. J. 85 (2007) 308.